SIMULATION OF THERMAL COMFORT IN SOCCER STADIA USING TRNSYS 17

Christian Frenzel[1], Sabine Gröger[2], Marion Hiller[1], Wolfgang Kessling[1], Katrin Müllner[1]
[1]TRANSSOLAR Energietechnik GmbH, Stuttgart, Germany
[2]Technische Universität München, Lehrstuhl für energieeffizientes und nachhaltiges Planen und Bauen, Munich, Germany

ABSTRACT

The Soccer World Cup in Qatar 2022 has started a discussion on thermal comfort in soccer stadia, particularly in hot and humid climates and their related energy consumption.

To evaluate the thermal comfort in such an environment a calculation algorithm for the so-called "perceived temperature" (PT), is incorporated into the TRNSYS 17 simulation package. In addition, an extended 3D MRT model is applied allowing detailed 3D modeling of longwave and shortwave solar radiation on a sensor depending on its location within an environment.

This paper presents the first study of different stadia types focusing on the effect of longwave and shortwave radiation on the thermal comfort. The results show that solar radiation striking a spectator causes a significant increase of the PT and the associated thermal stress level. Thermal comfort simulations enable planers to evaluate and optimize the design concept of stadia roofs including material properties.

INTRODUCTION

Stadia, exceptional in architecture and dimension, present a certain challenge in simulation. Especially, stadia with roof construction present a semi-outdoor space such that the applied comfort model must have the ability to model both an indoor situation with reflective surfaces and an outdoor environment with solar radiation.

In addition, to evaluate the thermal comfort in such a semi-outdoor environment, in hot and humid climates, requires that the comfort index considers humidity adaption.

Thermal comfort

"Thermal comfort is that condition of mind, which expresses satisfaction with the thermal environment" (ASHRAE Standard, 2004) or simply said the sensation of feeling neither too hot nor too cold. It is the moment when heat loss to the surroundings and heat production by the body balance and the body is in perfect equilibrium. Thermal comfort is however not the same as thermal neutrality. A person influenced by asymmetric temperature radiation though thermally neutral may still feel local discomfort.

This shows that air temperature alone as the indicator for heat or cold stress will not suffice to describe thermal comfort. The large number of parameters influencing thermal comfort can be broken down to seven fundamental variables. They can be further divided into environmental and personal factors. The first group, consisting of solar and infrared radiation, ambient air temperature, air velocity, and air humidity, represents meteorological data measured at the site of interest.

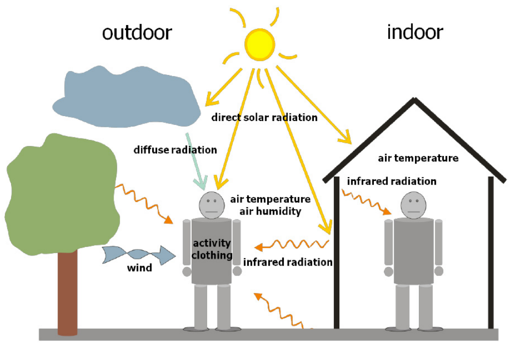

Figure 1 Human comfort parameters

Outdoor comfort evaluation is more complex. All environmental factors are highly dependent on location and surrounding must be taken into account.

The body's efforts to adapt to the meteorological aspects can be aided by behavioral measures: wearing adequate clothing (especially in the case of cold stress) or moving into the shade in the case of heat stress. The two behavioral or personal factors contributing to comfort are thus the metabolic rate describing the amount of internal heat production and the clothing index influencing the heat dissipation towards the environment.

Furthermore, achieving thermal comfort in a meteorologically defined environment is then the challenge of the body's internal heat production by metabolism and its thermophysiological regulation system. In hot climates the only possibility for the body to gain comfort is by vasodilatation and transpiration. This second becomes difficult in hot climates with a high humidity ratio preventing evaporation, as this leaves the body helpless without means of regulation. Cold stress on the other hand can be regulated by shivering and vasoconstriction.

Perceived Temperature (PT)

The 'perceived temperature'(PT) uses the concept of an equivalent temperature by applying the PMV value, which may have been corrected according to Gagge et. al (1986), to the air temperature of a standardised meteorological reference environment where the same perception of warm or cold (same PMV value) would occur as in the actual environment (VDI 3787, 2008). In the reference environment the wind velocity is reduced to a slight draught, and the mean radiant temperature is equal to the air temperature. The water vapour pressure is identical with the actual environment as far as it is not reduced by condensation. Perceived heat and cold is computed by means of the comfort equation by Fanger (1970) which is based on a complete heat budget model of the human body. The thermo-physiological assessment is made for a male, the "Klima Michel" (Jendritzky et al., 1990), aged 35 years, 1,75 m tall, weighing 75 kg. His work performance is 172,5 W which corresponds to a metabolic rate of 2,3 Met, and to walking ca. 4 km/h on flat ground. The assessment procedure is designed for a standard male choosing his clothing between summer and winter clothes, in order to gain thermal comfort as far as possible. (Summer clothes: 0,50 clo, winter clothes: 1,75 clo).

Thermal perception and thermo-physiological stress are evaluated according to Table 1 which shows the thermal perception to be expected for the respective perceived temperature, and the corresponding thermo-physiological stress. (VDI3787, 2008)

Table 1 Perceived temperature and thermal stress following VDI 3787 (2008)

Perceived temperature [°C]	Thermal perception	Thermo-physiological stress
PT ≥ 38	very hot	extreme heat stress
+32 ≤ PT < +38	hot	great heat stress
+26 ≤ PT < +32	warm	moderate heat stress
+20 ≤ PT < +26	slightly warm	slight heat stress
0 < PT ≤ +20	comfortable	comfort possible
-13 < PT ≤ 0	slightly cool	slight cold stress
-26 < PT ≤ -13	cool	moderate cold stress
-39 < PT ≤ -26	cold	great cold stress
PT ≤ -39	very cold	extreme cold stress

The influence of humidity on the PT calculation acc. to Gagge et al. (1986) can be seen in Figure 2. Here, the "operative temperature" – which is used for the standard PMV and denotes the mean of air temperature and mean of radiant temperature, weighted with the heat transfer coefficients for convection and radiation – is replaced by the "effective temperature" which additionally considers the enthalpy of skin damp with sweat and wet clothing.

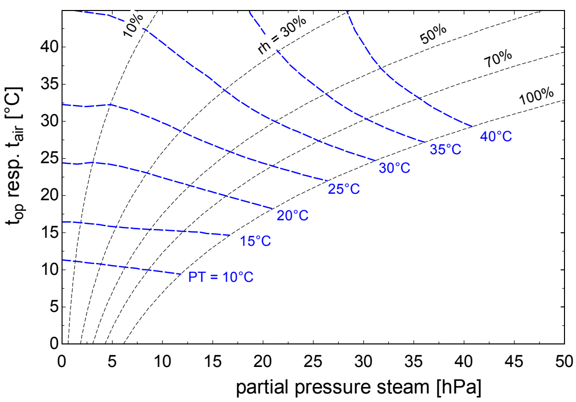

Figure 2 Mollier diagram with PT Isotherm for v_{air}= 1 m/s , Metabolic Rate=70 W/m², I_{cl} = 0.75 clo

The perceived temperature (PT) is used by the German Weather Service DWD to develop vivid maps and predictions of thermal comfort deals with the outdoor comfort.

MODELING IN TRNSYS17

TRNSYS 17 is a complete and extensible simulation environment for the transient simulation of thermal systems including multi-zone buildings. The package includes detailed radiation model for shortwave radiation distribution and longwave radiation exchange within an environment which is mandatory for detailed comfort modeling. The influence of short and longwave radiation are generally described by an index called the mean radiant temperature (MRT) which has to be determined for every possible situation as it depends on the person's orientation towards surrounding surfaces and the sun. The MRT in relation to a person in a given body posture and clothing placed at a given point in a room, is defined as that uniform temperature of black surroundings which will give the same radiant heat loss from the person as the actual case under study. (Fanger, 1970) This complicates the calculation of thermal comfort outside.

The detailed model of thermal comfort included in TRNSYS 17 is based on a MRT calculation restricted to longwave radiation only and therefore not applicable for stadia simulation. Instead an extended 3D MRT model (Hiller, M. et al., 2010) is applied allowing detailed modeling of longwave and shortwave solar radiation on a sensor depending on the location within an environment. Both models are explained in detail.

Detailed MRT Model of TRNSYS 17

For taking into account different emissivities of surrounding surfaces especially of low-e effects the MRT calculation has to include reflection. Therefore, so called Gebhart factors are applied. The Gebhart factor $G_{A\text{-}B}$ is defined as the part of the emissions of a surface A (or a differential surface element) that is absorbed on a surface B including all possible paths (multi-reflections). For further details see Aschaber et al. 2009. In the detailed model a sphere shaped so-called bulb thermometer with a diameter of 0.07m based on DIN EN ISO 7726 and 3787 is modelled. A bulb thermometer can be used to determine the mean radiant temperature in a room by measurement. The sphere simplifies to calculate the view factor of the sensor to surrounding surfaces and the validation procedure versus a “real (human) shaped” sensor.

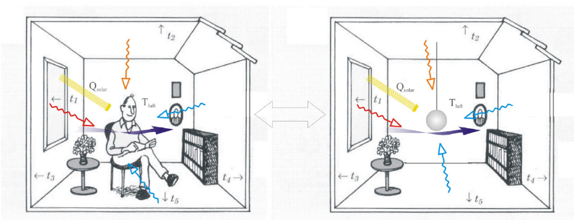

Figure 3 Modelling of the human body as a spherical sensor in the original environment

The sphere’s MRT can be used to approximate the mean radiant temperature of a more complex human body for most of the realistic situations. Particularly for seated persons view factors of the human body and a sphere match with very small deviations (Dillig, 2009). Compared to standing humans a sphere overestimates the influence of floor and ceiling on MRT. However, this does not create a remarkable error except for abnormally high temperature inhomogenities in a room.

If all surface temperatures of a thermal environment are known the mean radiant temperature is given by:

$$T_{MR}^{ir} = \left[\sum_{i=1}^{n} T_i^4 G_{s,i}^{ir} \right]^{1/4} \qquad (1)$$

With:

$G_{s,i}^{ir}$ the Gebhart factor from sensor surface s to surface i in the IR range

The equation is derived from Fanger’s definition of the mean radiant temperature based on longwave radiation. It is important to notice that the surface of the sensor is part of the radiation exchanging environment. Consequently its surface temperature T_s has to be known in order to evalute MRT according to equation (1).

The sensor surface temperature T_s can be obtained by the thermal equilibrium condition between convection and radiation driven heat fluxes:

$$\dot{Q}_s^{conv} + \dot{Q}_s^{ir} = 0 \qquad (2)$$

A detailed description of this calculation procedure can be found in the TRNSYS 17 manual (Klein et al., 2009).

Extended Detailed MRT Model

Since shortwave solar radiation has a major influence on the mean radiant temperature the existing model of the sensor was extended to the shortwave solar spectrum including direct, diffuse and reflected radiation effects. Therefore, the thermal equilibrium condition of equation (2) has to be extended by a direct solar and diffuse solar heat flux:

$$\dot{Q}_{dir}^{solar} + \dot{Q}_{diff}^{solar} + \dot{Q}_s^{ir} + \dot{Q}_s^{conv} = 0 \qquad (3)$$

Both solar heat fluxes have to include the primary as well as the reflected solar radiation. Therefore, a new set of Gebhart factors is computed for the shortwave spectrum and the fluxes can be described by

$$\dot{Q}_{dir}^{solar} = f_p A_s \alpha_s^{solar} i_n^{dir} + \sum_{i=1}^{n} I_i^{dir} \rho_i^{solar} G_{i,s}^{solar} \qquad (4)$$

$$\dot{Q}_{diff}^{solar} = \sum_{i=1}^{n} I_i^{diff} G_{i,s}^{solar} \qquad (5)$$

With:

f_p the projection factor of the sensor

A_s the sensor surface

α_s^{solar} the solar absorbance of the sensor

i_n^{dir} incident direct solar radiaton density on a surface perpendicular to the incident radiation direction

ρ_i^{solar} the solar reflectivity of a surface i

I_i^{dir} incident direct solar radiation on surface i

I_i^{diff} transmitted diffused radiation through surface I (=0 for opaque walls and >0 for windows)

$G_{i,s}^{solar}$ shortwave Gebhart factors from surface i to sensor surface s

Consequently, the total mean radiant temperature including infrared as well as solar effects can be obtained by:

$$T_{MR} = \left[\left(T_{MR}^{ir} \right)^4 + \frac{1}{\varepsilon_s^{ir} \sigma \cdot A_s} \left(\dot{Q}_{diff}^{solar} + \dot{Q}_{dir}^{solar} \right) \right]^{1/4} \quad (6)$$

For outdoor spaces, VDI 3787 gives an equation for the MRT including solar effects. However, this equation is valid only for perfectly black surrounding surfaces. The equation given by VDI can be derived from eq. (6) by setting all emissivity's to 1. A validation study of this model is given by Hiller, M. et. al. (2010).

Equation (6) allows computing mean radiant temperature of the sensor. To gain comparability to the more complex human body optical properties have to be fixed to specific values that represent the thermal relations at the human body surface. For a 0.07 m sized sphere an IR emissivity of 0.82 and solar absorbance of 0.53 were chosen (Dillig, M., 2009).

Additionally, the high intensity of direct solar radiation requires closer consideration of the differences in shape between the human body and the sensor. Direct solar heat flux depending on the projection factor f_p eq. (6) causes an important dependency of human MRT on solar altitude angle for a standing person.

Consequently, for a standing person the projection factor of the sphere, being constantly at 0.25, is replaced by the angle dependent projection factors of the human body given by VDI 3787 (2008). Thereby a correction of the direct solar heat flux is done. The low intensity diffuse and reflected solar radiation fluxes however are well approximated using the sphere as a human body representation.

IMPLEMENTATION INTO TRNSYS17

The previously described extended detailed model has been implemented as a prototype into TRNSYS 17 by Hiller et al., (2010).

In addition, the existing insolation calculations for direct radiation are extended to determine if a given point is sunlit (depending on external shading), and from which external windows it receives sunlight. The sunlit factors are written to an external file (*.IPM) which is read in by the multi-zone building model at the start of the simulation. (Hiller et al., 2010)

Since the standard package of TRNSYS offers operative temperature and PMV (predicted mean vote) as comfort indices an algorithm for PT calculation provided by VDI 3787 (2008) was linked to TRNSYS 17.

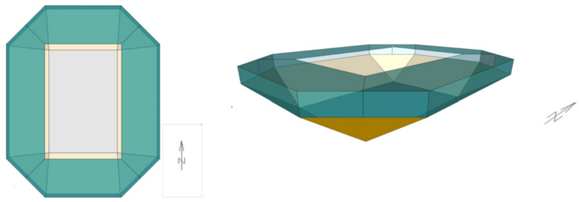

Figure 4 The basic stadium model in Trnsys3d: dome stadium with translucent membrane roof

SIMULATION MODEL

Since the study focuses on the effect of longwave and shortwave radiation on the thermal comfort, simplified assumptions for modeling the air movement were applied. The air velocity is assumed to be constant for all positions in the different stadium models although the structure greatly influences the air turbulences inside the stadium. Further analysis by computational fluid dynamics simulation could be used to evaluate air flows and varying wind reduction coefficient within the stadia. For the convective heat transfer a constant average wind speed of 4.4 m/s over the simulation period is assumed. For inside surfaces a wind reduction factor of 0.35 is used whereas for outside surfaces no wind reduction factor is applied. A constant infiltration rate of 26 ach was assumed.

Model 1: Dome Stadium with translucent membrane roof

The basic simulation model represents a typical dome stadium with a field size of 100m x 150m (see Figure 4). The stands are completely covered with a partly translucent membrane leaving the center part over the field open to the sky.

For creating the 3D model the user interface Trnsys3d, a plugin for Google SketchUp™, was used. Trnsys3d is also used to visualize simulation results in 3D.

The stadium is modeled as one (radiative) zone composed by different airnodes. One airnode representing the lower part with the stands and the field and other airnodes representing the upper roof section.

The ground floor and the external walls of the stands are built of 0.5 m concrete.

The roof membrane is modeled as a window with a solar transmittance of 10 % and an outside solar reflectance of 79 % and a frame ratio of 30 %.

The opening in the roof is modeled as a window with 100 % transmitted for shortwave solar and a surface temperature equal the sky temperature for longwave radiation exchange (no convection on inside surface).

The stands and the field are modeled by nine surfaces, but 196 sensor position for comfort evaluation. They are located at 1m height in the center of each section shown in Figure 5.

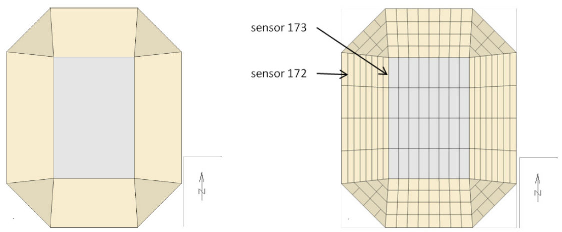

Figure 5 Left) Surface distribution for simulation and Right) surface distribution for determination of geopositions as well as illustration of simulated sensor temperatures

It is assumed that each of the sensor positions represents a single spectator sitting alone in the stadium. No additional internal loads are included.

Model 2: Open stadium

The open stadium type is typical for older stadia such as the Stade Velodrome in Marseille, France or the Cirtus Ball, Orlando, USA.

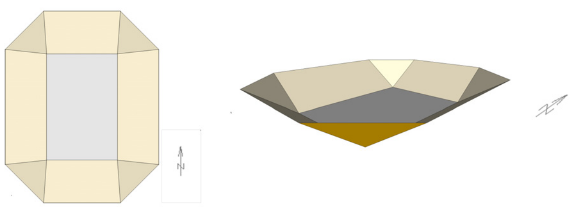

Figure 6 Open stadium model in Trnsys3d

Model 3: Completely covered stadium

The third stadium type to be compared is a hypothetical completely covered stadium, where even the center opening is closed by a membrane. This reduces solar radiation gains inside the whole stadium, but on the other hand natural turf would not grow. More often this type of stadium exists in combination with a movable roof. An example is the University of Phoenix Stadium, Arizona, USA or the new Wembley Stadium, GB.

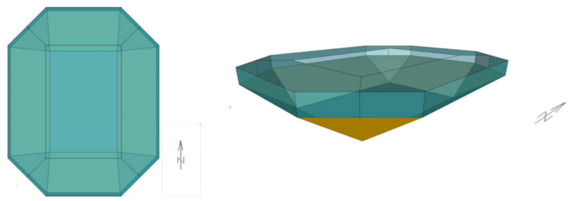

Figure 7 Completely covered stadium model in Trnsys3d

Model 4: Plaza

As a reference model an open plaza with a single sensor at height of 1 m in the middle was created.

Climate conditions

The simulations are performed for a Mediterranean environment using the IWEC climate data set of Marseille. Marseille has an annual mean temperature of 14.8 °C and a total radiation of 1545 kWh/m²/a .

For showing the resulting PT and MRT the authors choose July 14th with a maximum insolation of 935 W/m², 29 °C air temperature, and a humidity of approx. 11 g/kg. This day represents a typical summer day of this climate. The simulation period is from July 1st to 15th ensuring a warming up period of 13 days. Climate conditions are shown in Figure 8 – Figure 9.

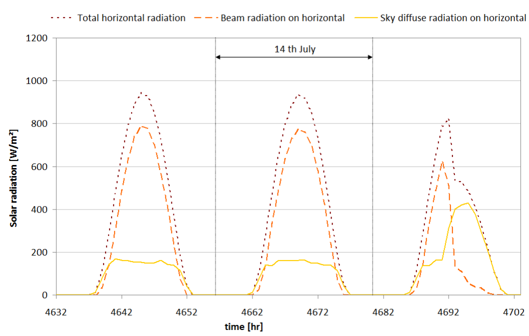

Figure 8 Total, direct and diffuse radiation on a horizontal plane from July 13 to July 15

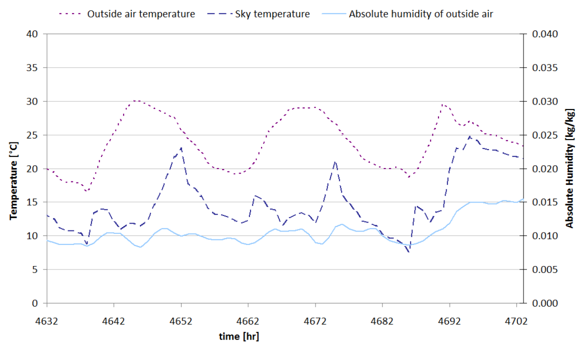

Figure 9 Outside air temperature, sky temperature and absolute humidity of outside air from July 13 to July 15

RESULTS AND DISCUSSION

Comfort evaluation of the dome stadium and an open plaza

Under the described climate conditions of Marseille the perceived temperature (PT) for the dome stadium as well as an open plaza is simulated.

For July 14th the resulting hourly values of the PT are shown in Figure 10. For the stadium, the resulting PT values of the comfort positions are mapped to the surface grid shown in Figure 5. The results of the plaza correspond to the square left of the stadium top view. The coloring scale is chosen from 22.5 °C increasing in 0.5 K steps to max. temperature of 35 °C. All data featuring colder PT than 22.5 °C or hotter then 35°C is black. In addition, the second scale visualizes the corresponding thermal perception according to VDI (light grey: range where comfort is possible, middle grey: slight heat stress, dark grey: moderate heat stress, black: great heat stress).

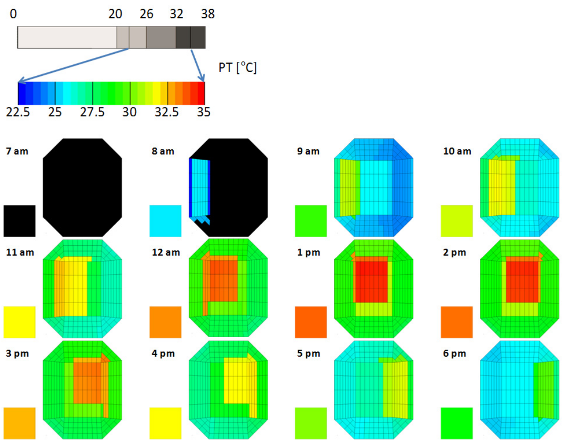

Figure 10 PT on July 14, 7 a.m. to 6 p.m. for the dome stadium and an open plaza (left square)

The results show that direct solar radiation through the opening in the membrane roof causes a significant increase of the PT. For example at noon, PT reaches 34 °C (great heat stress) in the unshaded center field and lower western stands while the shaded stands in the south east show a PT of 27 °C (moderate heat stress).

In the evening at 5 p.m. when most matches take place PT can still differ by 5 K with a PT of 26 °C on the shaded western stands and 31 °C in the sunlit east stands. This corresponds to moderate heat stress for spectators in the top eastern stands, while the spectator in the west feel slightly warm only.

Comparing the results of the dome stadium to the ones of an open plaza, the plaza's PT doesn't reach as high as values as in the stadium. This is due to the longwave radiation cooling by an unobstructed view to the cooler sky temperature, whereas in the stadium the view to the cooler sky is limited to the central opening in the membrane roof.

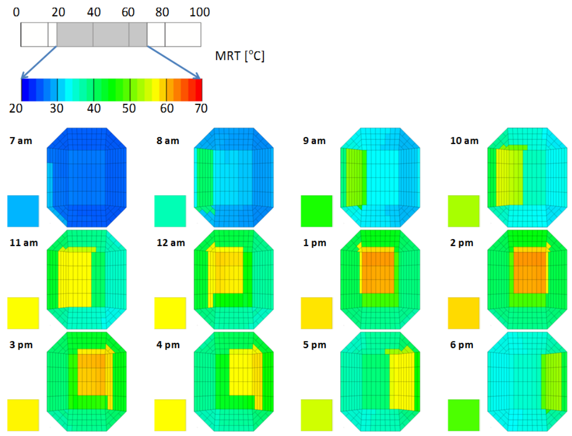

Figure 11 MRT on July 14, 7 a.m. to 6 p.m. for the dome stadium and an open plaza (left square)

The MRT is the parameter of the PT calculation that accounts for impact of longwave and short wave radiation. Figure 11 shows the corresponding hourly MRT for July 14th. As expected the MRT shows the same patterns but with a higher daily amplitude. The temperature range is from 22 °C to a peak of 64 °C at 2 p.m.

For sensor 173 located at the lower western stands close to the field (see Figure 5) the results of a three day period are shown in Figure 12. Besides the PT and MRT of the sensor the influencing surface temperatures like the roof temperature, the tribune temperature, the sky temperature and also the air temperature are included.

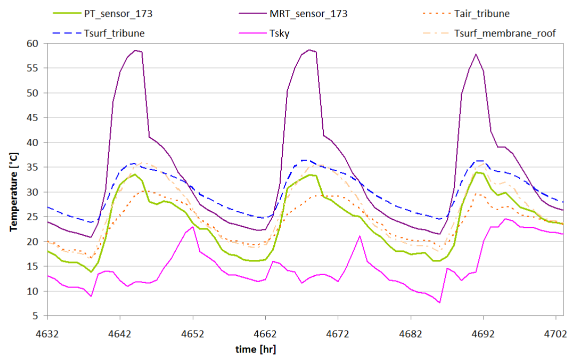

Figure 12 PT and MRT of sensor 173 and influencing surface temperatures from July 13 to July 15.

The stand surface temperature as well as the membrane roof temperature rise up to 35 °C whereas the air temperature is close to the ambient temperature. As previously mentioned this is related to the assumption of a constant infiltration rate of 26 ach. When the sensor is stroked by direct radiation both PT and MRT show a steep rise and when the sensor is shaded at 2 p.m. a steep decrease.

For studying the effect of solar radiation further detailed, another simulation without solar radiation on the sensor 173 was performed. Thereby, the influencing surface and air temperatures are the same as in the previous simulations. As shown in Figure 13 the solar radiation causes an increase in MRT of up to 25 K. This shows the importance of taking into account short wave radiation into the comfort index calculation under these boundary conditions.

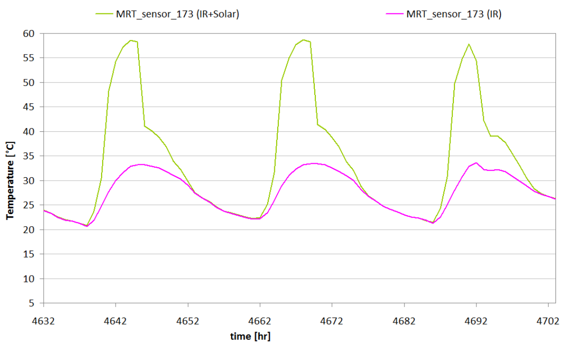

Figure 13 MRT with and without shortwave radiation of sensor 173 from July 13 to July 15.

Comfort evaluations for different roof constructions

The access of solar radiation is mainly influenced by the roof construction and has an impact on the comfort situation within a stadium. In addition to the dome stadium an open and a completely covered stadium are simulated (see Figure 6 and 7). The resulting PT and MRT at 9 a.m., 11 a.m., 2 p.m. and 5 p.m are shown in Figure 14 and 15, respectively. The results show very different levels of thermal comfort for the three stadia models under the defined boundary conditions.

As expected the lowest overall PT is provided by the completely covered stadium. The PT does not exceed 30 °C (moderate heat stress) and therewith it is only slightly higher than the maximum air temperature of 29 °C. Due to the effective reduction of solar gains the dependency of the PT on the daytime is greatly reduced. In addition, the comfort difference with respect to location within the stadium is very small.

The open stadium shows the highest PT values of up to 35.5 °C (the black patches indicate that the maximum range of 35°C is exceeded.) In addition, due to the high solar gains during daytime the PT indicates great heat stress on the stands from most of the time.

The thermal comfort of the dome stadium is somewhere in between the open and completely covered stadium. The roof construction increases the comfort of the spectators significantly compared to the open stadium, but it also reaches a PT of 34 °C in the unshaded center field and the lower western stands.

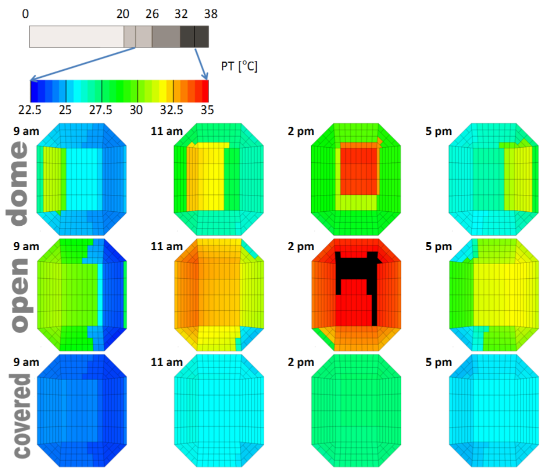

Figure 14 PT for July 14 showing the three variants dome, open and completely covered stadium

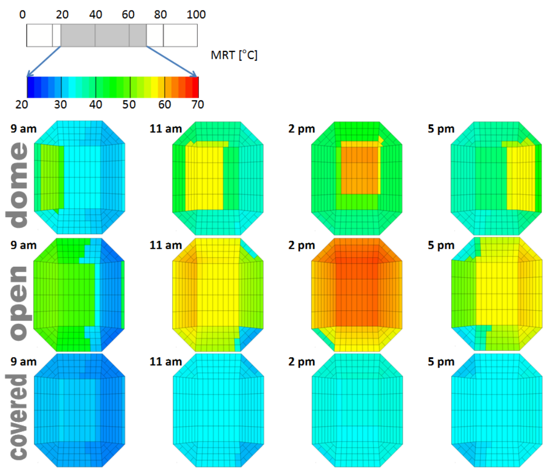

Figure 15 MRT for July 14 showing the three variants dome, open and completely covered stadium

CONCLUSIONS AND OUTLOOK

For this study an algorithm of PT calculation was successfully integrated into TRNSYS17. In addition, an extended 3D model for MRT evaluation taking into account solar radiation on a sensor was applied.

The results of this first study showed that solar radiation striking a spectator causes a significant increase of the PT and the associated thermal stress level. For example for a dome stadium at noon, PT reaches 34 °C (great heat stress) in the unshaded center field and lower western stands while the shaded stands in the south east show a PT of 27 °C (moderate heat stress).

A comparison of three different stadia types showed that for the Mediterranean climate a dome stadium increases the comfort for the spectators significantly compared to an open stadium. In addition, the performed simulations showed that thermal comfort simulation enables planners to evaluate and optimize their design concept of stadia roofs including material properties.

In a further step active measures like air treatment, floor cooling or evaporative cooling could be integrated in the model evaluating the influence on the thermal comfort.

Since the focus of the study was set to the effect of longwave and shortwave radiation on the thermal comfort, simplified assumption for modeling the air movement were applied. Further analysis by CFD tools should be used to evaluate local air flows and varying the wind reduction coefficient within the stadia. These results could be integrated in the thermal model.

REFERENCES

Aschaber, J et al., 2009, TRNSYS17: New Features of Multi-zone Building Bodel, 11th International Building Performance Simulation Association Conference, Glasgow Scotland.

ASHRAE Standard 55 – 2004, 2004, Thermal Environmental Conditions for Human Occupancy. Atlanta GA : American Society of Heating, Refrigerating and Air-Conditioning Engineers, Inc..

Dillig, M. Diplomarbeit, 2009, Entwicklung von Sensoren zur Messung der operativen Temperatur in unterschiedlichen Umgebungen. TUM : Lehrstuhl für Thermodynamik.

Fanger, P.O., 1970, Thermal Comfort Analyis and Applications in Environmental Engineering, Copenhagen.

Gagge, A.P., Fobelet, A.P., Berglund, P.E., 1986, A standard predictive index of human response to the thermal environment. ASHRAE Trans. 92, pp. 709–731.

Hiller, M., Aschaber, J., and Dillig, M., 2010, Integration of low-e surfaces and shortwave solar radiation into human comfort calculation in TRNSYS 17. BauSIM 2010 conference, Vienna, Austria.

Jendritzky, G., Menz G., Schirmer H., Schmidt-Kessen W., 1990, Methodik zur raumbezogenen Bewertung der thermischen Komponente im Bioklima des Menschen (Fortgeschriebenes Klima-Michel-Modell). - Beitr. Akad. Raumforsch. Landespl. 114.

Klein, S.A. et al., 2009, TRNSYS 17: A Transient System Simulation Program, SEL, University of Wisconsin, Madison USA.

VDI 3787 Blatt 2 : 2008 - 11, 2008, Umweltmeteorologie - Methoden zur human-biometeorologischen Bewertung von Klima und Lufthygiene für die Stadt- und Regionalplanung - Teil 1: Klima Berlin: Beuth Verlag.